



The non-conservative distribution pattern of organic matter in Rajang, a tropical river with peatland in its estuary

Zhuoyi Zhu^{1*}, Joanne Oakes², Bradley Eyre², Youyou Hao¹, Edwin Sien Aun Sia³, Shan Jiang¹,
 Moritz Müller³, Jing Zhang¹

1. State Key Laboratory of Estuarine and Coastal Research, School of Oceanography, East China
 Normal University, Shanghai, 200241, China

2. Centre for Coastal Biogeochemistry, School of Environment, Science and Engineering, Southern
 Cross University, Lismore NSW, 2480, Australia

3. Swinburne University of Technology, Faculty of Engineering, Computing and Science, Jalan
 Simpang Tiga, Kuching, 93350, Sarawak, Malaysia

*corresponding author: Z.Y. Zhu, zyzhu@sklec.ecnu.edu.cn; zhu.zhuoyi@163.com

Abstract

South-east Asian peatland-draining rivers have attracted much attention due to their high
 dissolved organic carbon (DOC) yield and high CO₂ emissions under anthropogenic activities. In
 August 2016, we carried out a field investigation of the Rajang river and estuary, a tropical system
 located in Sarawak, Malaysia. The Rajang has peatland in its estuary while the river basin is covered
 by tropical rainforest. DOC $\delta^{13}\text{C}$ in the Rajang ranged from -28.7‰ to -20.1‰ and a U-shaped trend
 from river to estuary was identified. For particulate organic carbon (POC), the $\delta^{13}\text{C}$ ranged between
 -29.4‰ to -31.1‰ in the river and a clear increasing trend towards more $\delta^{13}\text{C}$ -enriched with higher
 salinity existed in the estuary. In the estuary, there was a linear conservative dilution pattern for
 dissolved organic matter composition (as quantified by D/L amino acids enantiomers) plotted
 against DOC $\delta^{13}\text{C}$, whereas when plotted against salinity dissolved D/L amino acids enantiomers
 values were higher than the theoretical dilution value. Together, these data indicate that the addition
 of DOC in estuary (by peatland) not only increased the DOC concentration, but also altered its
 composition, by adding more bio-degraded, ¹³C-depleted organic matter into the bulk dissolved
 organic matter. Alteration of organic matter composition (adding of more degraded subpart) was
 also apparent for the particulate phase, but patterns were less clear. The Rajang was characterized
 by DOC/DON ratios of 50 in the river section, with loss of DON in the estuary increased the ratio
 to 140, suggesting the unbalanced export pattern for organic carbon and nitrogen, respectively.
 Under anthropogenic activities, further assessment of organic carbon to nitrogen ratio is needed.

Keyword

Amino acids enantiomers, DOC, POC, stable carbon isotope, Rajang, peatland



36 1. Introduction

37 Fluxes and cycling of organic matter (OM) in rivers and estuaries are important influences on
38 global biogeochemical cycles and climate change. In river basins, vascular plants are the ultimate
39 sources of organic matter (Hedges and Man, 1979), but algae, moss and bacteria are also important
40 (Hernes et al., 2007). As well as providing a source of OM, bacteria may also strongly modify the
41 composition of organic matter within a river and its resistance to degradation. The lability of organic
42 matter determines how rapidly organic carbon will be transformed into inorganic carbon (CO₂),
43 which can vary from hours to millions of years. The lability of organic matter therefore plays a role
44 in determining whether organic matter is either a source or a sink of carbon in the atmosphere (Zhang
45 et al., 2018). Based on ¹⁴C of organic carbon, Mayorga et al. (2005) determined that the degradation
46 of recently synthesized organic matter in the river basin was the main reason Amazonian river
47 waters were supersaturated in CO₂, and hence the a source of atmospheric CO₂. This highlights the
48 potential importance of organic matter stability for carbon cycling within river systems. Nitrogen is
49 another important element in organic matter, which is not independent from carbon, but instead is
50 closely combined with carbon in various chemical compounds (like amino acids). Due to the nature
51 of these specific compounds, the behavior of bulk carbon and nitrogen can differ substantially. In
52 basins with peatland, the leaching of DOC is related to the status of peatland (disturbed vs
53 undisturbed), whereas the leaching of dissolved organic nitrogen (DON) is controlled by the soil
54 inorganic nitrogen content (Kalbitz and Geyer, 2002). The different leaching mechanisms of organic
55 carbon and nitrogen indicates that the comparison of these two elements would deepen our
56 understanding of organic matter cycles.

57 Tropical south-east Asian rivers play an important role in both dissolved and particulate organic



58 matter export (Baum et al., 2007; Huang et al., 2017; Müller et al., 2016). Located in Sarawak,
59 Malaysia (Fig. 1a), the turbid Rajang river (hereafter refer to as the Rajang) is the longest river in
60 Malaysia. The Rajang flows through tropical rainforest, and peatland and mangroves are distributed
61 in the estuary (downstream of Sibü; Fig. 1b). A dam was constructed in the upper reaches of the
62 Rajang in 2015, but the total suspended matter (TSM) in the river downstream of Kapit remains at
63 100 – 200 mg/L in recent years (Müller-Dum et al., 2019). Dilution of terrestrial organic matter in
64 the adjacent coast is expected, while turbid river water strongly limits apparent organic matter
65 photo-degradation within the river and estuary, leaving the stage of fluvial organic matter alteration
66 to bacteria utilization and abiotic process like desorption/adsorption between particulate and
67 dissolved phase (Martin et al., 2018). Further, dissolved oxygen is negatively related to pCO₂, likely
68 due to in-stream heterotrophic respiration (Müller-Dum et al., 2019). In the Rajang brackish estuary,
69 where peatland is located, addition of peatland DOC into river water is suggested by the non-
70 conservative mixing pattern of DOC with increasing salinity (Martin et al., 2018), whereas removal
71 of DON in the Rajang estuary is suggested by nitrogen stable isotopes (Jiang et al., 2019).

72 While stable isotopes of carbon and nitrogen are useful tools for tracing organic matter, amino
73 acids (AAs) are the most important organic carbon and nitrogen carriers that have been chemically
74 identified, accounting for up to ~100% of the particulate nitrogen in aquatic environments, and up
75 to nearly half of the particulate organic carbon pool (Jennerjahn et al., 2004). Due to the selective
76 removal and accumulation of certain amino acids, amino acids are important biomarkers in early
77 diagenesis, allowing quantification of organic matter lability/resistance (Dauwe and Middelburg,
78 1998; Kaiser and Benner, 2009). With the exception of glycine, amino acids are chiral. L forms of
79 amino acids are from animals, plants and plankton, whereas D forms mainly come from bacteria,



80 and are key chemical compounds in peptidoglycan, which forms the basic structure of bacterial cell
81 membranes (Vollmer et al., 2008). Due to the key role of bacteria in OM alteration and early
82 diagenesis, D-AAAs (D forms AAAs) tend to accumulate during OM degradation. A higher ratio of D-
83 to L-AAAs (D/L ratio) therefore indicates more that OM is more refractory (Davis et al., 2009). As a
84 non-protein amino acid, accumulation of GABA (γ -aminobutyric acid) is also highly related to
85 OM degradation (Davis et al., 2009). Conversely, a lower D/L ratio and GABA% indicates that OM
86 is relatively less degraded, and hence more labile. In river waters, elevated D-AAAs also indicates
87 the presence of soil humic substances, which is a product of bacteria and their detritus (Kimber et
88 al., 1990).

89 Tropical rivers are dominated by refractory (or bio-degraded) organic matter, yet labile OM is
90 also known to play a role in river carbon cycles (Mayorga et al., 2005). It is hence expected that the
91 fluvial organic matter in the river would be a mixture of labile organic matter (that can be respired
92 to support $p\text{CO}_2$) and refractory terrestrial organic matter (that will be diluted/degraded after
93 entering the sea (Martin et al., 2018), while in the estuary there would be addition of dissolved OM
94 from peatland/mangrove (Dittmar et al., 2001b; Müller et al., 2016). Previous studies of OM in
95 south-east Asian rivers mainly focused on its bulk concentrations, ages, or optical properties (Martin
96 et al., 2018 and ref. therein). The use of biomarker approaches has been very limited (Baum et al.,
97 2007; Gandois et al., 2014). Given the processes described above and their potential contribution to
98 the carbon (Müller-Dum et al., 2019) and nitrogen cycles (Jiang et al., 2019), it is somewhat
99 surprising that there has been limited application of amino acid approaches, including D-AAAs, to
100 investigate organic matter composition and the role of estuarine peatland/mangrove in OM
101 regulation (Jennerjahn et al., 2004). South-east Asian rivers are subject to multiple stressors due to



102 increasing anthropogenic activities in both their riverine (e.g., damming, logging/secondary
103 plantation) and estuarine sections (e.g., drainage, and oil palm plantations) (Hooijer et al., 2015).
104 AAs enantiomers and carbon/nitrogen isotopes have the ability to provide molecular level evidence
105 for the impact of these stressors on carbon and nitrogen cycling and bulk biogeochemistry, as well
106 as insight into the mechanisms underlying such changes.

107 In this study, we carried out a field investigation in the Rajang in August 2016, from Kapit to
108 S1 station, located on the coast of the South China Sea adjacent to the Rajang (Fig. 1b). AAs
109 enantiomers and $\delta^{13}\text{C}$ of DOC were used to elucidate the succession of organic matter
110 sources/composition from the fresh water to the estuarine sections of the Rajang. Our aim was to
111 address the following questions: 1) Given that peatland contributes additional DOC to fluvial DOC
112 (Müller et al., 2016), does the composition of dissolved OM change from river to estuary? 2) Do
113 changes in organic nitrogen mirror changes in organic carbon? 3) And hence what is the role of
114 peatland/mangroves on OM composition and lability in the Rajang? Globally, rivers in low latitudes
115 receive much less attention relative to temperate and polar rivers (36 vs. 958 studies)(Cloern et al.,
116 2014), while they could equally important in carbon cycle (Cloern et al., 2014). Our work, together
117 with other tropical studies, would enrich the understandings for organic carbon and nitrogen cycles
118 in tropical rivers/estuaries.

119

120 **2. Materials and methods**

121 All abbreviations, together with the amino acids measured in this study, are listed in table 1.

122 **2.1 Brief background**

123 The Rajang river and estuary is located in Sarawak, Malaysia. The climate is wet year-round,



124 but the main precipitation typically occurs in winter (November to February). Climate is influenced
125 by El Niño-Southern Oscillation (ENSO) and Madden-Julian Oscillation. In August 2016, the
126 discharge was estimated as 2440 m³/s, in comparison with an annual mean discharge of 4000 m³/s
127 for 2016 and 2017 (Müller-Dum et al., 2019).

128 Based on salinity, Sibul is regarded as the boundary of the fresh and estuarine water of the
129 Rajang (Fig. 1b). In this work all samples with a salinity of 0 were regarded as fresh water, while
130 samples with salinity >0 were regarded as estuarine. In the estuary, there are several branches,
131 namely Igan, Lassa, Paloh, and Rajang itself (Fig. 1b). Since water in all these branches are from
132 Rajang river (i.e., upstream of Sibul), in this work all these branches are regarded as the Rajang
133 estuary. Peatland and mangroves are commonly distributed in the estuary (shown in Fig. 1b) while
134 tropical rainforest is widely distributed upstream of Sibul (not shown in Fig. 1b). The peatland is
135 under strong pressure of draining and change of use for oil palm, while in the basin logging and
136 secondary growth is very common (Hooijer et al., 2015). Compared with other peatland-draining
137 tropical blackwater rivers, the Rajang is more like a turbid tropical rainforest river (Müller-Dum et
138 al., 2019), but with notable peatland/mangrove in its estuary (Fig. 1b).

139 2.2 Field sampling

140 The field work was carried out in August 2016. The sampling stations covered from Kapit (the
141 upper most station in this study) to S1 on the coast. At each station, a pre-cleaned and sample-rinsed
142 bucket was used to collect surface water from the center of the channel in a boat. After sample
143 collection, pretreatment was done immediately on board in the boat. For DOC and its stable carbon
144 isotope ratios ($\delta^{13}\text{C}$), water samples were collected by syringe filtering (pre-combusted Whatman
145 GF/F; 0.7 μm) approximately 30 ml of sample water into a pre-combusted 40 ml borosilicate vial.



146 Samples were preserved with five drops of concentrated phosphoric acid and sealed with a lid
147 containing a Teflon-coated septa. For total dissolved amino acids (TDAA), water samples were
148 filtered through a 0.4 μm nylon filter. For particulate OM samples (TSM, POC, POC- $\delta^{13}\text{C}$, PN and
149 PN- $\delta^{15}\text{N}$, and total particulate amino acids (TPAA)), suspended particles were concentrated onto
150 glass fiber membrane (pre-combusted Whatman GF/F; 0.7 μm). The GF/F filters were folded and
151 packed in pre-combusted aluminum. All samples were immediately stored frozen (-20°C) until
152 analysis. A portable meter (Aquaread, AP-2000) was used to obtain conductivity/salinity,
153 temperature, dissolved oxygen and pH.

154 2.3 Laboratory analyses

155 Concentrations and $\delta^{13}\text{C}$ of DOC were measured via continuous-flow wet oxidation isotope-
156 ratio mass spectrometry using an Aurora 1030W total organic carbon analyzer coupled to a Thermo
157 Delta V IRMS (Oakes et al. 2010). Glucose of known isotopic composition dissolved in He-purged
158 Milli-Q was used as a standard to correct for drift and to verify sample concentrations and $\delta^{13}\text{C}$
159 values. Reproducibility for concentrations and $\delta^{13}\text{C}$ was $\pm 0.2 \text{ mg l}^{-1}$ and $\pm 0.4 \text{ ‰}$. DOC
160 concentrations and $\delta^{13}\text{C}$ were measured at the Centre for Coastal Biogeochemistry at Southern Cross
161 University (Lismore, Australia). For the determination of POC, samples (GF/F glass fiber filter)
162 were freeze-dried and analyzed with a CHNOS analyzer (Model: Vario EL III) after removing the
163 inorganic carbon by reaction with HCl vapor. For PN, a similar procedure like POC was followed,
164 but no acid was used in pre-treatment. The detection limit for POC was $7.5 \times 10^{-6} \text{ g}$, with precision
165 better than 6%, based on repeated determinations (Zhu et al., 2006). The POC- $\delta^{13}\text{C}$ and PN- $\delta^{15}\text{N}$
166 were determined using a DELTAplus/XL isotopic ratio mass spectrometer (Finnigan MAT Com.
167 USA) interfaced with a Carlo Erba 2500 elemental analyzer. The standard for $\delta^{13}\text{C}$ was PDB and



the precision of the analysis was $\pm 0.2\%$. For $\delta^{15}\text{N}$, the standard was air and precision was $\pm 0.3\%$.

Total hydrolyzable AAs were extracted and analyzed following the method of Fitznar et al., (1999) with slight modifications (Zhu et al., 2014). Briefly, samples were first hydrolyzed with HCl at 110°C . After pre-column derivatization with o-Phthaldialdehyde (OPA) and N-Isobutyl-L/D-cysteine (IBLC/IBDC), AAs and their enantiomers were analyzed using an HPLC (Agilent 1200) comprising of an online vacuum degasser, a quaternary pump, an auto-sampler, a thermostatted column and a fluorescence detector (excitation 330 nm, emission 445 nm). The analytical column was a Phenomenex Hyperclone column (BDS C18, $250 \times 4\text{mm}$, $5\mu\text{m}$) with a corresponding pre-column. To eliminate the influence of racemization of L-type AAs in the hydrolysis process, the concentration of D/L AAs measured in actual samples was corrected according to the formula obtained by Kaiser and Benner (2005). The detection limit for glycine (Gly) and individual AAs enantiomers were in the lower picomolar level. Asx and Glx were used for aspartic acid + asparagine and glutamic acid + glutamine, respectively (Table 1), as the corresponding acids are formed via deamination during hydrolysis.

A few samples (e.g., TDAA in S1 station) were not measured due to instrument hardware problem. And hence the measured particulate and dissolved sample stations did not exactly match.

184

185 3. Results

In August 2016, the TSM concentration in the Rajang ranged from 22 mg/L (mean for the fresh water section) to 161 mg/L (mean for the estuarine section) (Table 2). Throughout the system DOC concentrations exceeded POC concentrations. DOC and POC in the fresh water section averaged 337 μM and 86 μM , and in the estuarine section 345 μM and 64 μM , respectively (Table 2). While



190 DOC concentration was slightly higher in the estuary than in the fresh water (Table 2), a maximum
 191 of both DOC and POC can be found at around salinity 15 to 20 in the estuary (Fig. 2).

192 DOC $\delta^{13}\text{C}$ ranged from -28.7‰ to -20.1‰ (Table 2). A U-shaped trend from fresh water
 193 section to estuary section can be identified for DOC $\delta^{13}\text{C}$, with one outlier from the Rajang main
 194 stream at a salinity of 5 (S2 station; Fig. 3a). The minimum value of DOC $\delta^{13}\text{C}$ (bottom of the U)
 195 was detected at a salinity of ~10 (Fig. 3a). For particulate OM, $\delta^{13}\text{C}$ ranged between -29.4‰ to -
 196 31.1‰ in the fresh water section. In the estuary section, there was a clear increasing trend with
 197 increasing salinity, from -30‰ (S=1.1) to values close to -24‰ (S>30) (Fig. 3b).

198 In the fresh water section, the mean TDAA and TPAA concentrations were 0.3 μM and 2.5
 199 μM , respectively (Table 3). For TDAA, the AA carbon yield (the carbon from AA divided by bulk
 200 DOC or POC, in %) in both fresh water and estuary sections were very similar, namely 0.40% and
 201 0.38% (mean), respectively (Table 3), whereas AA nitrogen yield was higher in the estuary (11%)
 202 than in the fresh water section (4.8%) (Table 3). For TPAA, there was little difference between the
 203 fresh water and estuary sections in AA carbon yield (13.5% and 16.8%, respectively) and nitrogen
 204 yield (66% and 62%, respectively) (Table 3).

205 With respect to individual AA compounds, in both dissolved and particulate phase, Gly, Glx,
 206 Ala and Asx were the most abundant four AAs. These four AAs together accounted for 66% of
 207 TDAA and 47% of TPAA in the fresh water section, 59% of TDAA and 48% of TPAA in the estuary.
 208 The non-protein AA GABA was detected in trace amounts, but was accumulated in the dissolved
 209 phase relative to the particulate phase, as indicated by the higher GABA% in the dissolved phase
 210 (Table 3). GABA% decreased from 2% (fresh water section mean) to 1.3% (estuarine section mean)
 211 in the dissolved phase, and decreased from 0.7% (fresh water section mean) to 0.4% (estuarine



section mean) in the particulate phase (Table 3). In the estuary, GABA% in the dissolved phase remained stable (~1.5%) in brackish water (salinity 5 to 20) and quickly dropped to <1% where salinity was over 30 (Fig. 4a). Most of the GABA% dots were above the theoretical dilution line (Fig. 4a). In the particulate phase, there was an overall decrease in GABA% with increasing salinity within the estuary (Fig. 4b).

As for the AA enantiomers, the D/L ratio of AA in the dissolved phase averaged 12% for both fresh water and estuarine section. The most abundant D-form AAs in the dissolved phase were Glx and Asx. For the particulate phase, the D/L ratio of AA was much lower, decreasing from a mean of 4.4% in the fresh water section to a mean of 3.3% in the estuary (Table 3). And patterns in the variation of D/L Glx (Fig. 5) along with conductivity/salinity gradient in the Rajang were similar to those for GABA% (Fig. 4) for both dissolved and particulate phase. For example, for dissolved phase, a similar platform can be identified at salinity range of 5 to 20 (Fig. 5a), whereas for particulate phase the decreasing pattern along with salinity is very clear in the estuary (Fig. 5b). Also, for dissolved phase in the estuary, all the data were above the theoretical dilution line for D/L Glx.

227

228 4. Discussion

229 4.1 Distribution patterns of OM composition

230 *Dissolved OM*

Terrestrial OM usually has a more negative $\delta^{13}\text{C}$ value (–32‰ to –26‰ for C3 plants), whereas marine OM has more positive value values ($\delta^{13}\text{C}$, ~ –20‰) values (Lamb et al., 2006; Mayorga et al., 2005). Overall, the very negative $\delta^{13}\text{C}$ values for DOC (<–26‰) in the river part of the Rajang



indicates that the OM had a very clear C3 plant source (e.g., mangroves and oil palms (Jennerjahn et al., 2004; Lamade et al., 2009; Wu et al., 2019)), whereas DOC $\delta^{13}\text{C}$ values $> -24\text{‰}$ in the estuary (salinity >30) suggest a mixture of terrestrial and marine OM (Fig. 3a). The most depleted $\delta^{13}\text{C}$ values for DOC occurred at a salinity of 10 (Fig. 3a). Above this salinity, the influence of marine OM became more overwhelming, and the bulk DOC $\delta^{13}\text{C}$ signal was more enriched (Fig. 3a).

Among samples in the fresh water section, the sample of most enriched DOC- $\delta^{13}\text{C}$ value (S10 and S15; DOC- $\delta^{13}\text{C}$: -25‰ ; Fig. 3a) although initially appearing to be outliers, were characterized by very elevated D/L amino acids ratios (Fig. 6a). This was particularly the case for the sample from S10 (the upper most station in this study; Fig. 1b), which showed a maximum D/L Glx ratio of 0.57 (Fig. 6a). In addition, these samples from S10 and S15 also showed a higher D/L ratio for Asp (S10: 0.49, S15: 0.38; figure not shown) when compared to all fresh water or estuary samples (mean: 0.34; Table 3). On land, D form amino acids can be derived from abiotic racemization process (which requires a very long time scale) by which L form amino acids slowly changed into their corresponding D form (Schroeder and Bada, 1976). More significantly in contemporary environments, D form amino acids are widely synthesized by bacteria during their cell membrane construction (Schleifer and Kandler, 1972). D/L Glutamic acid and D/L Aspartic acid ratios of pure peptidoglycan (*Staphylococcus aureus*, Gram-positive) are 0.49 and 0.30, respectively (Amon et al., 2001). Though $\delta^{13}\text{C}$ values for bacteria in the Rajang remains unclear, bacteria have been reported to have $\delta^{13}\text{C}$ values from -12‰ to -27‰ (Lamb et al., 2006). Contribution of OM derived from bacteria may therefore explain the relatively enriched $\delta^{13}\text{C}$ values observed at inland S10 station and S15. A possible OM source at these stations is soil humic substances, which are expected to be under strong impact of bacteria, and have a high contribution of D-form amino acids (Dittmar et al.,



256 2001a). A more depleted pattern of DOC $\delta^{13}\text{C}$ from mountain to lowland is suggested to be due to
 257 dilution and mixing with younger OM in the lowland (Mayorga et al., 2005). This is consistent with
 258 our findings that, depleted pattern of riverine DOC $\delta^{13}\text{C}$ within the fresh water section was
 259 corresponding to a lowering D/L ratio pattern, which indicates the dilution with less degraded OM
 260 (Fig. 6a). Whether the dissolved samples with elevated D/L ratio and relatively positive $\delta^{13}\text{C}$ in the
 261 fresh water section (S10 and S15; Fig. 6a) reflect the presence of soil humic substances, or instead
 262 reflect the direct presence of bacteria, requires further study.

263 In the estuarine section, it was very clear that terrestrial bio-degraded OM (indicated by
 264 elevated D/L ratios and more negative $\delta^{13}\text{C}$) is diluted with more labile OM (lower in D/L ratio but
 265 more positive $\delta^{13}\text{C}$)(Fig. 6a). However, this apparent dilution trend became very vague (or showed
 266 no trend) when D/L ratio was plotted against salinity (Fig. 5a). This was also confirmed by the
 267 GABA% distribution pattern which showed a platform-like pattern at a salinity between 5 and 20
 268 (Fig. 4a). Though TDAA at S1 is missing, the composition of TDAA at S2 (salinity = 31.2) was
 269 very typical of marine OM (i.e., very low D/L ratio and relatively enriched DOC- $\delta^{13}\text{C}$; see Fig. 6a).
 270 Hence in the estuary there is a conservative distribution pattern for dissolved OM when plotted
 271 against $\delta^{13}\text{C}$ (Fig. 6a) but such pattern disappeared when plotted against salinity (Fig. 4a&5a). The
 272 location above the conservative dilution line of all OM data in the brackish estuary (salinity between
 273 10 and 25; Fig. 4a&5a), indicates that the OM in the estuarine section was more degraded than
 274 theoretically expected. The combination of degraded OM with the observed DOC concentration
 275 increase in the estuary (345 μM in the estuary vs. 337 μM in the fresh water section; or Fig. 2b),
 276 suggests the addition of degraded DOC to the Rajang. Non-conservative dissolved OM behavior in
 277 the estuary has previously been reported based on an optical approach (Martin et al., 2018), and



minimal OM alteration during estuarine transport was suggested (Martin et al., 2018). Hence, it is reasonable that changes in dissolved OM composition (Fig. 4a&5a) may largely take place in land/estuary (e.g., in pore waters of soil) and impact the Rajang riverine dissolved OM via leaching from soils.

Particulate OM

As for dissolved OM, depleted POC- $\delta^{13}\text{C}$ in the river part of the Rajang indicated the strong influence of terrestrial OM (e.g., C3 plant Dittmar et al., 2001b) whereas in the estuary, particulate OM was diluted with marine particulate OM, as indicated by the seawards enrichment of $\delta^{13}\text{C}$ (Fig. 3b). In the sediment, a clear woody angiosperm C3 plants as the OM source is found based on a lignin approach (Wu et al., 2019), and similar increases in carbon and nitrogen isotopes in suspended particles in brackish water have also been observed in other estuaries (Cifuentes et al., 1996; Raymond and Bauer, 2001). Unlike dissolved OM, there were no samples with unusually enriched $\delta^{13}\text{C}$ values in the fresh water section (Fig. 6b&c). D/L Glx ratio in the fresh water section is higher when compared with that in the estuary section (Table 3), and overall, when compared with dissolved OM, particulate OM basically became more labile when transporting seawards, as indicated by its composition shift along with salinity (Fig. 4b&5b) or isotope (Fig. 6b&c).

Although particulate OM had a lower D/L ratio than dissolved OM (Fig. 6), it should be noted that this does not mean dissolved OM is more aged or degraded than particulate OM. Rather, as observed in other estuaries (Dittmar et al., 2001a), bacteria and their detritus simply tend to accumulate in the dissolved phase, relative to the particulate phase.

4.2 Different fate of bulk organic carbon and nitrogen

Leaching of DOC and DON from peatlands is driven by difference mechanisms; whereas DOC



300 release is related to the status of peatland (pristine vs. degraded), DON release is determined by the
 301 DIN content of peatland soil (Kalbitz and Geyer, 2002). In the Rajang, bulk DOC and DON
 302 concentrations were not coupled, as suggested by the DOC/DON ratio variation pattern (Fig. 7).
 303 The average DOC concentration in the estuary part was slightly higher (345 μM) than in the river
 304 part (337 μM ; Table 3), which indicates the addition of DOC in the estuary. In comparison, the
 305 removal of DON in the estuary is suggested (Jiang et al., 2019).

306 In the Rajang, non-conservative dilution behavior from optical properties was observed for
 307 estuarine DOC (Martin et al., 2018), which is consistent with other peatland-draining rivers in
 308 Sarawak (Müller et al., 2016). The contribution of marine sources to dissolved OM is reflected in
 309 the increasing DOC- $\delta^{13}\text{C}$ in the estuary part (Fig. 3a). Peatland, however, is known for its high
 310 contribution to fluvial DOC and has been suggested to contribute to the DOC in the Rajang (Martin
 311 et al., 2018). In peatland-draining rivers west of the Rajang, the DOC concentration endmember can
 312 be as high as 3690 μM (Müller et al., 2015). Under such high DOC background, a simple three-
 313 point mixing model (i.e., a model that based on 1 observed fresh water DOC endmember, 2 peatland
 314 DOC endmember and 3 calculated fresh water DOC endmember) suggests that peatland-DOC
 315 addition accounts for 3% of the fluvial DOC in the Saribas river and 15% in the Lupar river (Müller
 316 et al., 2016). Assuming that peatland in the Rajang estuary has a comparable endmember DOC
 317 concentration to other peatland in Sarawak (i.e., 3690 μM ; Müller et al., 2015), and given our
 318 observed Rajang fresh water DOC endmember value of 337 μM (DOC concentration at S5 station)
 319 and a marine DOC endmember of 238 μM (S1 station), a similar model approach suggests peatland
 320 DOC addition contributed 4% of the Rajang fluvial DOC, which is comparable to Saribas river and
 321 much lower than Lupar river (Müller et al., 2016). In the meantime, as mentioned in the previous



section, there is a non-conservative dilution pattern, with dissolved OM in the estuary part more degraded than expected based on simple dilution with a marine endmember (Fig. 4a&5a). Hence it is reasonable that peatland not only contributed to the fluvial DOC in concentration (Martin et al., 2018), but also modified the dissolved OM composition (more bio-degraded) in the estuary. In another tropical river study, mangrove in the estuary exerted a stronger influence on fluvial dissolved OM than hinterland vegetation (Dittmar et al., 2001b). This is consistent with the Rajang, for which estuarine processes apparently impact the dissolved OM in terms of both DOC concentration (by increasing the bulk amount) and composition (by adding bio-degraded DOC). The estuarine dissolved OM showed higher bio-degraded feature (e.g., elevated GABA% and D/L ratio; Fig. 4a&5a), but this subpart may be photolabile (Martin et al., 2018). When TSM decreases and light condition in the water column becomes good (e.g., entering the sea), photodegradation is expected (Martin et al., 2018). Other oceanic degradation mechanisms include the priming effect (Bianchi, 2011). The fate of the terrestrial OM in the sea requires further study. As we lack the DON concentration endmember in peatland, peatland impact on DON in the estuary is not estimated.

In contrast to DOC, which was apparently added to the estuary, DON was removed, contributing to a remarkable increase of dissolved inorganic nitrogen in the estuary (Jiang et al., 2019). In the fresh water section, the nitrate concentration was not related to the ratio of D/L dissolved AAs, nor related to dissolved GABA% (Fig. 8), and in the estuarine section, nitrate was not related to D/L AAs but it indeed was related to GABA% in the estuarine section (Fig. 8b). This indicates that fluvial nitrate in the fresh water section was not derived from remineralization of fluvial organic matter in the river channel, but more likely from other sources (e.g., leaching of soil). In the estuarine section, there may be some DON transformation occurred (Jiang et al., 2019), while



the leaching from soil process still cannot be eliminated (Fig. 8). For particulate phase, no relation can be found between nitrate and particulate OM composition (figure not shown).

The atomic DOC/DON in Rajang averaged 50 in the river part, and increased to 140 (mean value) in the estuary part (Fig. 7). Although the DOC/DON ratio was much higher when compared to other tropical peatland river waters (around 10; Sjögersten et al., 2011), the ratio is comparable with other peatland-draining rivers in Sarawak like the Lupar, Saruba and Maludan rivers (Müller et al., 2015; Müller et al., 2016), which all enter the South China sea. The ratio is also within the reported C/N ratio of peatland and leaves (Müller et al., 2016). For the Amazon river, the DOC versus total nitrogen ratio ranges from 27 to 52 (Hedges et al., 1994). Given their reported total nitrogen includes inorganic nitrogen, the DOC/DON ratio for the Amazon river would be even higher. Under the background of such high C/N ratios (e.g., 50), transformation of DON to DIN in the estuary further enhanced the high DOC/DON ratio (to 140), and hence a deficiency in terrestrial organic nitrogen output is expected. We noted that dissolved inorganic nitrogen for Rajang is on the order of 10 μ M, comparable to DON (Jiang et al., 2019). Terrestrial nitrogen output is an important source for coastal primary production (Jiang et al., 2019), but peatland-impacted rivers may have relatively lower nitrogen input to the South China Sea when compared with their very high river basin DOC yields (Baum et al., 2007). On one hand, logging and secondary growth has been found to play a negative role in the nitrogen output efficiency of forest soils (Davidson et al., 2007). On the other hand, disturbed tropical peatlands could release more DOC in comparison to an undisturbed site (Moore et al., 2013) while the DOC/DON ratio may also decrease along with disturbance of peatland (Kalbitz and Geyer, 2002). Given that secondary growth in river basin and anthropogenic disturbance of peatland (e.g., drainage and conversion for oil palm) are both common



366 (Hooijer et al., 2015), changes of DOC/DON ratios in the Rajang are complex and further
367 assessment is needed in the future.

368

369 5. Summary and Conclusion

370 In August 2016 in the Rajang, we observed that dissolved OM composition (as D/L Glx ratio)
371 was conservatively diluted along with increasing DOC $\delta^{13}\text{C}$, indicating that the sources of dissolved
372 OM have a very conservative impact on the OM composition. When D/L Glx ratio was plotted
373 against salinity (as is usually done for an estuarine OM behavior check in many studies), such linear
374 conservative dilution pattern disappeared (Fig. 4a&5a). This implies that the addition of DOC in the
375 estuary (peatland/mangrove) had an impact on dissolved OM composition, adding more bio-
376 degraded OM, and resulting in data above the theoretical dilution line (Fig. 4a&5a). For particulate
377 OM, though the data was variable, the overall decreasing GABA% or ratio along with salinity was
378 much clearer relative to that of dissolved OM (Fig. 4b&5b). Particulate D/L Glx ratio in the estuary
379 was usually lower when compared with that in the fresh water section (Fig. 6b&c), whereas for
380 dissolved OM, the majority of the samples in the estuary had a D/L Glx ratio similar to that in the
381 fresh water (Fig. 6a). The difference in OM composition between fresh water and estuarine section
382 suggests that dissolved OM became more degraded while particulate OM became less degraded in
383 the estuary.

384 The Rajang is characterized by DOC/DON ratios of 50 in the fresh water section, and the
385 further loss of DON in the estuary increased the ratio to 140. Peatland draining and
386 logging/secondary growth are reported to have conflicting impacts on carbon and nitrogen cycling
387 (Davidson et al., 2007; Moore et al., 2013), which may increase fluvial DOC and limit basin nitrogen



output, resulting in even larger DOC/DON. Mismatch in carbon and nitrogen loss from tropical rivers due to anthropogenic activities plays a role in material cycle in both land and marine systems, enhancing the tropical river as a direct carbon source to atmosphere while for nitrogen change and its further feedback on carbon cycle needs further monitoring and assessment.

At last, this work is based on a dry season investigation (August). Though the seasonality for Rajang OM may be moderate (Martin et al., 2018), for biomarkers like amino acids enantiomers further investigation in the wet season is needed.

Acknowledgements

We thank captain and crew of the boat, as well as other colleagues on board during the field work. We thank colleagues and students in both Swinburne University of Technology (Sarawak Campus) and in State Key Lab of Estuarine and Coastal Research/East China Normal University. We thank Aazani Mujahid in University Malaysia Sarawak for her help and hospitality during our stay in Malaysia. This work is funded by the National Key Research and Development Program of China (2018YFD0900702), MOHE FRGS 15 Grant (FRGS/1/2015/WAB08/SWIN/02/1) in Malaysia, ARC Linkage Grant LP150100519 in Australia, a SKLEC Open Research Fund (SKLEC-KF201610) and ‘111’ project in SKLEC/ECNU from the Ministry of Education of China and State Administration of Foreign Experts Affaires of China.

References

- Amon, R. M. W., Fitznar, H. P., and Benner, R.: Linkages among the bioreactivity, chemical composition, and diagenetic state of marine dissolved organic matter, *Limnology and Oceanography*, 46, 287-297, 2001.
- Baum, A., Rixen, T., and Samiaji, J.: Relevance of peat draining rivers in central Sumatra for the riverine input of dissolved organic carbon into the ocean, *Estuarine, Coastal and Shelf Science*, 73, 563-570, 2007.
- Bianchi, T. S.: The role of terrestrially derived organic carbon in the coastal ocean: A changing paradigm



- and the priming effect, *Proceedings of the National Academy of Sciences*, 108, 19473-19481, 2011.
- Cifuentes, L. A., Coffin, R. B., Solorzano, L., Cardenas, W., Espinoza, J., and Twilley, R. R.: Isotopic and Elemental Variations of Carbon and Nitrogen in a Mangrove Estuary *Estuarine Coastal and Shelf Science*, 43, 781-800, 1996.
- Cloern, J. E., Foster, S. Q., and Kleckner, A. E.: Phytoplankton primary production in the world's estuarine-coastal ecosystems, *Biogeosciences*, 11, 2477-2501, 2014.
- Dauwe, B. and Middelburg, J. J.: Amino acids and hexosamines as indicators of organic matter degradation state in North Sea sediments, *Limnology and Oceanography*, 43, 782-798, 1998.
- Davidson, E. A., de Carvalho, C. J. R., Figueira, A. M., Ishida, F. Y., Ometto, J. P. H. B., Nardoto, G. B., Saba, R. T., Hayashi, S. N., Leal, E. C., Vieira, I. C. G., and Martinelli, L. A.: Recuperation of nitrogen cycling in Amazonian forests following agricultural abandonment, *Nature*, 447, 995-998, 2007.
- Davis, J., Kaiser, K., and Benner, R.: Amino acid and amino sugar yields and compositions as indicators of dissolved organic matter diagenesis, *Organic Geochemistry*, 40, 343-352, 2009.
- Dittmar, T., Fitznar, H. P., and Kattner, G.: Origin and biogeochemical cycling of organic nitrogen in the eastern Arctic Ocean as evident from D- and L-amino acids, *Geochimica et Cosmochimica Acta*, 65, 4103-4114, 2001a.
- Dittmar, T., Lara, R. J., and Kattner, G.: River or mangrove? Tracing major organic matter sources in tropical Brazilian coastal waters, *Marine Chemistry*, 73, 253-271, 2001b.
- Fitznar, H. P., Lobbes, J. M., and Kattner, G.: Determination of enantiomeric amino acids with high-performance liquid chromatography and pre-column derivatisation with o-phthalaldehyde and N-isobutyrylcysteine in seawater and fossil samples (mollusks), *Journal of Chromatography A*, 832, 123-132, 1999.
- Gandois, L., Teisserenc, R., Cobb, A. R., Chieng, H. I., Lim, L. B. L., Kamariah, A. S., Hoyt, A., and Harvey, C. F.: Origin, composition, and transformation of dissolved organic matter in tropical peatlands, *Geochimica et Cosmochimica Acta*, 137, 35-47, 2014.
- Hedges, J. I., Cowie, G. L., Richey, J. E., Quay, P. D., Benner, R., Mike, S., and Forsberg, B. R.: Origins and processing of organic matter in the Amazon River as indicated by carbohydrates and amino acids, *Limnology and Oceanography*, 39, 743-761, 1994.
- Hedges, J. I. and Man, D. C.: The characterization of plant tissues by their lignin oxidation products, *Geochimica et Cosmochimica Acta*, 43, 1803-1807, 1979.
- Hernes, P. J., Robinson, A. C., and Aufdenkampe, A. K.: Fractionation of lignin during leaching and sorption and implications for organic matter "freshness", *Geophysical Research Letters*, 34, 2007.
- Hooijer, A., Vernimmen, R., Visser, M., and Mawdsley, N.: Flooding projections from elevation and subsidence models for oil palm plantations in the Rajang delta peatlands, Sarawak, Malaysia, *Deltares report 1207384*, 76 pp., 2015.
- Huang, T. H., Chen, C. T. A., Tseng, H. C., Lou, J. Y., Wang, S. L., Yang, L., Kandasamy, S., Gao, X., Wang, J. T., Aldrian, E., Jacinto, G. S., Anshari, G. Z., Sompongchaiyakul, P., and Wang, B. J.: Riverine carbon fluxes to the South China Sea, *Journal of Geophysical Research: Biogeosciences*, 122, 1239-1259, 2017.
- Jennerjahn, T. C., Ittekkot, V., Klöpper, S., Adi, S., Purwo Nugroho, S., Sudiana, N., Yusmal, A., Prihartanto, and Gaye-Haake, B.: Biogeochemistry of a tropical river affected by human activities in its catchment: Brantas River estuary and coastal waters of Madura Strait, Java, Indonesia, *Estuarine, Coastal and Shelf Science*, 60, 503-514, 2004.
- Jiang, S., Müller, M., Jin, J., Wu, Y., Zhu, K., Zhang, G., Mujahid, A., Rixen, T., Muhamad, M. F., Sia,



- 458 E. S. A., Jang, F. H. A., and Zhang, J.: Dissolved inorganic nitrogen in a tropical estuary at Malaysia:
459 transport and transformation, *Biogeosciences Discuss.*, 2019, 1-27, 2019.
- 460 Kaiser, K. and Benner, R.: Biochemical composition and size distribution of organic matter at the Pacific
461 and Atlantic time-series stations, *Marine Chemistry*, 113, 63-77, 2009.
- 462 Kaiser, K. and Benner, R.: Hydrolysis-induced racemization of amino acids, *Limnology and*
463 *Oceanography: Methods*, 3, 318-325, 2005.
- 464 Kalbitz, K. and Geyer, S.: Different effects of peat degradation on dissolved organic carbon and nitrogen,
465 *Organic Geochemistry*, 33, 319-326, 2002.
- 466 Kimber, R. W. L., Nannipieri, P., and Ceccanti, B.: The degree of racemization of amino acids released
467 by hydrolysis of humic-protein complexes: Implications for age assessment, *Soil Biology and*
468 *Biochemistry*, 22, 181-185, 1990.
- 469 Lamade, E., Setiyo, I. E., Girard, S., and Ghashghaie, J.: Changes in $^{13}\text{C}/^{12}\text{C}$ of oil palm leaves to
470 understand carbon use during their passage from heterotrophy to autotrophy, *Rapid Communications in*
471 *Mass Spectrometry*, 23, 2586-2596, 2009.
- 472 Lamb, A. L., Wilson, G. P., and Leng, M. J.: A review of coastal palaeoclimate and relative sea-level
473 reconstructions using $\delta^{13}\text{C}$ and C/N ratios in organic material, *Earth-Science Reviews*, 75, 29-57, 2006.
- 474 Müller-Dum, D., Warneke, T., Rixen, T., Müller, M., Baum, A., Christodoulou, A., Oakes, J., Eyre, B.
475 D., and Notholt, J.: Impact of peatlands on carbon dioxide (CO_2) emissions from the Rajang River and
476 Estuary, Malaysia, *Biogeosciences*, 16, 17-32, 2019.
- 477 Müller, D., Warneke, T., Rixen, T., Müller, M., Jamahiri, S., Denis, N., Mujahid, A., and Notholt, J.:
478 Lateral carbon fluxes and CO_2 outgassing from a tropical peat-draining river,
479 *Biogeosciences*, 12, 5967-5979, 2015.
- 480 Müller, D., Warneke, T., Rixen, T., Müller, M., Mujahid, A., Bange, H. W., and Notholt, J.: Fate of
481 terrestrial organic carbon and associated CO_2 and CO emissions from two Southeast Asian estuaries,
482 *Biogeosciences*, 13, 691-705, 2016.
- 483 Martin, P., Cherukuru, N., Tan, A. S. Y., Sanwlani, N., Mujahid, A., and Müller, M.: Distribution and
484 cycling of terrigenous dissolved organic carbon in peatland-draining rivers and coastal waters of Sarawak,
485 Borneo, *Biogeosciences*, 15, 6847-6865, 2018.
- 486 Mayorga, E., Aufdenkampe, A. K., Masiello, C. A., Krusche, A. V., Hedges, J. I., Quay, P. D., Richey, J.
487 E., and Brown, T. A.: Young organic matter as a source of carbon dioxide outgassing from Amazonian
488 rivers, *Nature*, 436, 538-541, 2005.
- 489 Moore, S., Evans, C. D., Page, S. E., Garnett, M. H., Jones, T. G., Freeman, C., Hooijer, A., Wiltshire, A.
490 J., Limin, S. H., and Gauci, V.: Deep instability of deforested tropical peatlands revealed by fluvial
491 organic carbon fluxes, *Nature*, 493, 660, 2013.
- 492 Raymond, P. A. and Bauer, J. E.: Use of ^{14}C and ^{13}C natural abundances for evaluating riverine,
493 estuarine, and coastal DOC and POC sources and cycling: a review and synthesis, *Organic Geochemistry*,
494 32, 469-485, 2001.
- 495 Schleifer, K. H. and Kandler, O.: Peptidoglycan types of bacterial cell walls and their taxonomic
496 implications, *Bacteriological Reviews*, 36, 407-477, 1972.
- 497 Schroeder, R. A. and Bada, J. L.: A review of the geochemical applications of the amino acid
498 racemization reaction, *Earth-Science Reviews*, 12, 347-391, 1976.
- 499 Sjögersten, S., Cheesman, A. W., Lopez, O., and Turner, B. L.: Biogeochemical processes along a
500 nutrient gradient in a tropical ombrotrophic peatland, *Biogeochemistry*, 104, 147-163, 2011.
- 501 Vollmer, W., Blanot, D., and de Pedro, M.: Peptidoglycan structure and architecture, *FEMS Microbiology*



502 Review, 32, 149-167, 2008.
 503 Wu, Y., Zhu, K., Zhang, J., Müller, M., Jiang, S., Mujahid, A., Muhamad, M. F., and Sia, E. S. A.:
 504 Distribution and degradation of terrestrial organic matter in the sediments of peat-draining rivers,
 505 Sarawak, Malaysian Borneo, Biogeosciences Discuss., 2019, 1-37, 2019.
 506 Zhang, C. L., Dang, H. Y., Azam, F., Benner, R., Legendre, L., Passow, U., Polimene, L., Robinson, C.,
 507 Suttle, C. A., and Jiao, N. Z.: Evolving paradigms in biological carbon cycling in the ocean, National
 508 Science Review, 5, 481-499, 2018.
 509 Zhu, Z. Y., Wu, Y., Zhang, J., Dittmar, T., Li, Y., Shao, L., and Ji, Q.: Can primary production contribute
 510 non-labile organic matter in the sea: Amino acid enantiomers along the coast south of the Changjiang
 511 Estuary in May, Journal of Marine Systems, 129, 343-349, 2014.
 512 Zhu, Z. Y., Zhang, J., Wu, Y., and Lin, J.: Bulk particulate organic carbon in the East China Sea: Tidal
 513 influence and bottom transport, Progress in Oceanography, 69, 37-60, 2006.
 514
 515



516 Table 1. Measured amino acids (the L- and D- enantiomers are not listed) and all abbreviations in
 517 this study. Note that glycine has no enantiomer.

name	abbreviations
organic matter	OM
dissolved organic carbon	DOC
dissolved organic nitrogen	DON
total suspended matter	TSM
amino acid	AA
total hydrolysable dissolved amino acids	TDAA
total hydrolysable particulate amino acids	TPAA
Alanine	Ala
Arginine	Arg
Asparagine	Asx
Aspartic acid	Asx
Glutamine	Glx
Glutamic acid	Glx
Glycine	Gly
Isoleucine	Ile
Leucine	Leu
Lysine	Lys
Methionine	Met
Phenylalanine	Phe
Serine	Ser
Threonine	Thr
Tryptophan	Trp
Tyrosine	Tyr
Valine	Val
γ - aminobutyric acid	GABA

518
 519



Table 2. TSM, DOC, POC and stable carbon isotopes in the freshwater and estuary of the Rajang
 (mean (min-max)).

	unit	Fresh water	Estuary
TSM	mg/L	61 (22 - 126)	73 (25 - 161)
DOC	μM	337 (217 - 658)	345 (214 - 587)
DOC δ ¹³ C	‰	-26.7 (-27.7 - -25.0)	-26.1 (-28.7 - -20.1)
POC	μM	86 (46 - 125)	64 (22 - 153)
	%	1.9 (1.2 - 2.5)	1.0 (0.6 - 1.9)
POC δ ¹³ C	‰	-30.1 (-31.1 - -29.4)	-26.7 (-30.1 - -23.8)

Table 3 The Rajang AAs result (mean (min-max)) in August 2016 (*total D/TDAA means total D
 form AA versus TDAA, the same for total D/TPAA)

		unit	Fresh water	Estuary
dissolved	TDAA	nM	317 (131 - 486)	523 (212 - 2320)
	TDAA carbon yield	%	0.40 (0.08 - 0.65)	0.38 (0.29 - 0.53)
	TDAA nitrogen yield	%	4.8 (1.3 - 15)	11 (5.4 - 18)
	GABA	%	2.0 (1.3 - 4.1)	1.3 (0.15 - 1.9)
	total D/total TDAA*	%	12 (8 - 15)	12 (3 - 14)
	D/L Glx		0.35 (0.16 - 0.57)	0.32 (0.07 - 0.42)
	D/L Asx		0.34 (0.23 - 0.48)	0.34 (0.08 - 0.42)
particulate	TPAA	μM	2.5 (1.4 - 3.6)	2.0 (1.1 - 3.7)
	TPAA carbon yield	%	14 (9.5 - 19)	17 (11 - 24)
	TPAA nitrogen yield	%	66 (36 - 82)	62 (30 - 100)
	GABA%	%	0.7 (0.6 - 0.9)	0.4 (0.2 - 0.8)
	total D/total TPAA*	%	4.4 (3.6 - 5.2)	3.3 (2.4 - 5.0)
	D/L Glx		0.09 (0.08 - 0.10)	0.06 (0.04 - 0.08)
	D/L Asx		0.04 (0.03 - 0.05)	0.05 (0.03 - 0.11)



Figure caption

Figure 1. Study area and sampling stations. a) Location of Sarawak, Malaysia; and b) the Rajang with its estuary/river mouth background shown. Samples upstream of Sibu showed 0 salinity while downstream of Sibu showed salinity >0 . Hence from Sibu to Kapit is regarded as the fresh water section, and downstream of Sibu is regarded as the estuarine section.

Figure 2. Distribution pattern of (a) TSM, (b) DOC and (c) POC along with conductivity/salinity in the Rajang. The location of salinity = 0 is at Sibu (Fig. 1b). The legend indicates the branches that the samples were from and marine corresponds to S1 station.

Figure 3. Distribution pattern of (a) DOC $\delta^{13}\text{C}$ and (b) POC $\delta^{13}\text{C}$ along with conductivity/salinity in the Rajang. The legend indicates the branches that the samples were from and marine corresponds to S1 station.

Figure 4. GABA% distribution pattern from fresh water to estuary in the Rajang: a) dissolved and b) particulate. The legend indicates the branches that the samples were from and marine corresponds to S1 station.

Figure 5. D/L ratio of Glx from fresh water to estuary in the Rajang: a) dissolved and b) particulate. The legend indicates the branches that the samples were from and marine corresponds to S1 station.

Figure 6. D/L ratio of AAs (as Glx) plotted against a) DOC $\delta^{13}\text{C}$ b) POC $\delta^{13}\text{C}$, and c) PN $\delta^{15}\text{N}$.

Figure 7. DOC/DON ratio distribution pattern along with salinity in the Rajang. For fresh water and estuary, the mean DOC/DON value was 50 and 140, respectively. DON is from Jiang et al., (2019)

Figure 8. Dissolved OM composition (a: D/L Glx, b: GABA%) and its relation with nitrate. Nitrate is derived from Jiang et al., (2019).

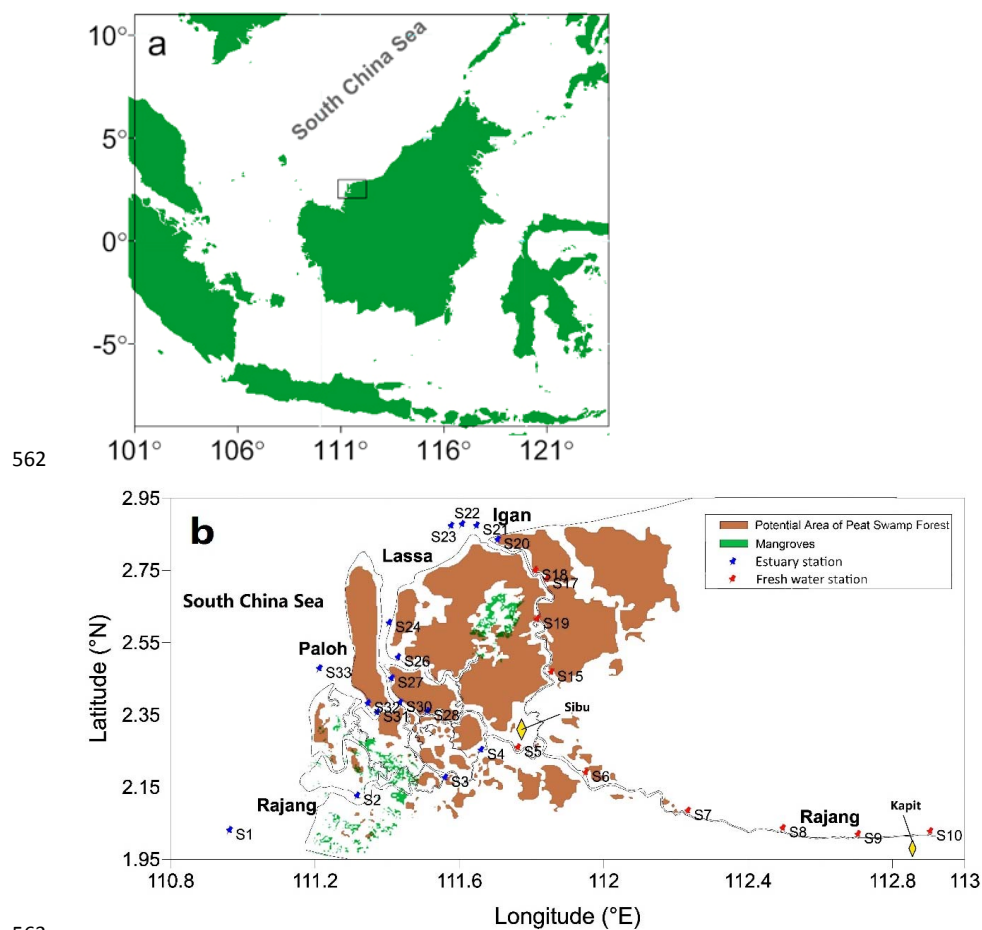


Figure 1. Study area and sampling stations. a) Location of Sarawak, Malaysia; and b) the Rajang with its estuary/river mouth background shown. Samples upstream of Sibu showed 0 salinity while downstream of Sibu showed salinity >0 . Hence from Sibu to Kapit is regarded as the fresh water section, and downstream of Sibu is regarded as the estuarine section.

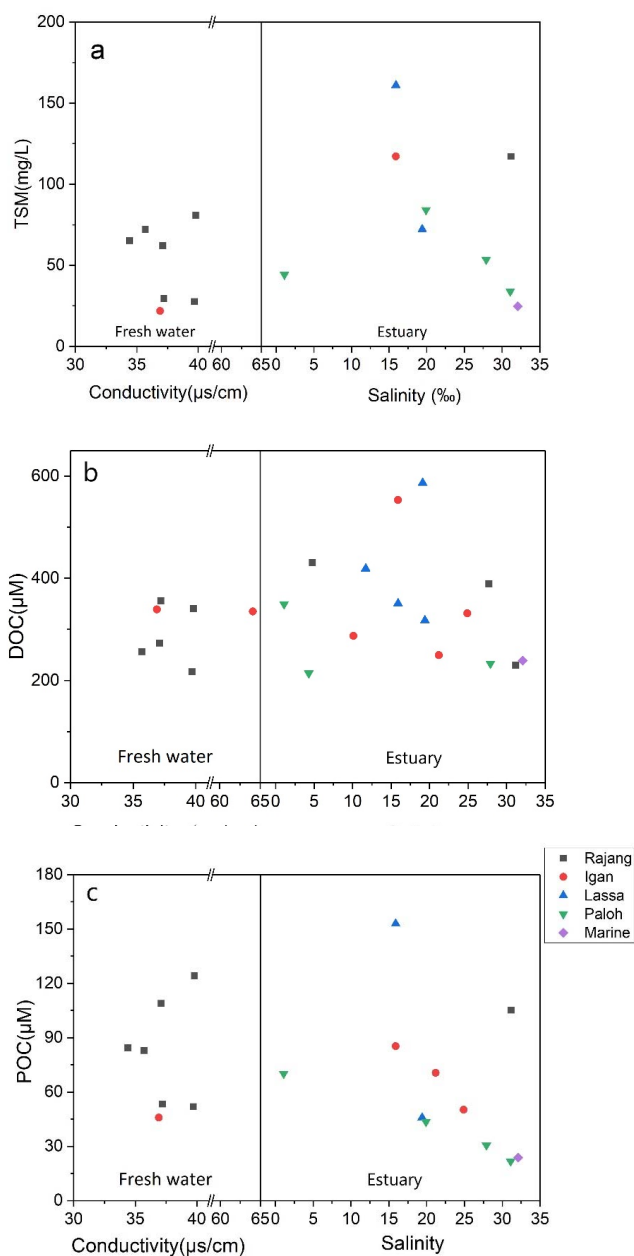
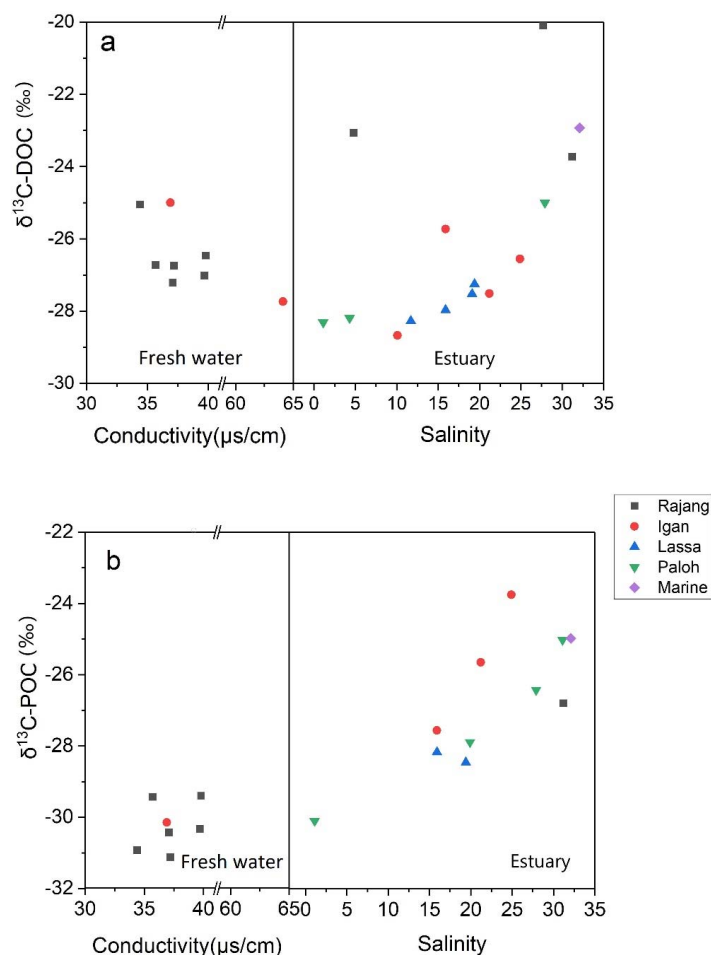


Figure 2. Distribution pattern of (a) TSM, (b) DOC and (c) POC along with conductivity/salinity in the Rajang. The location of salinity = 0 is at Sibul (Fig. 1b). The legend indicates the branches that the samples were from and marine corresponds to S1 station.



578



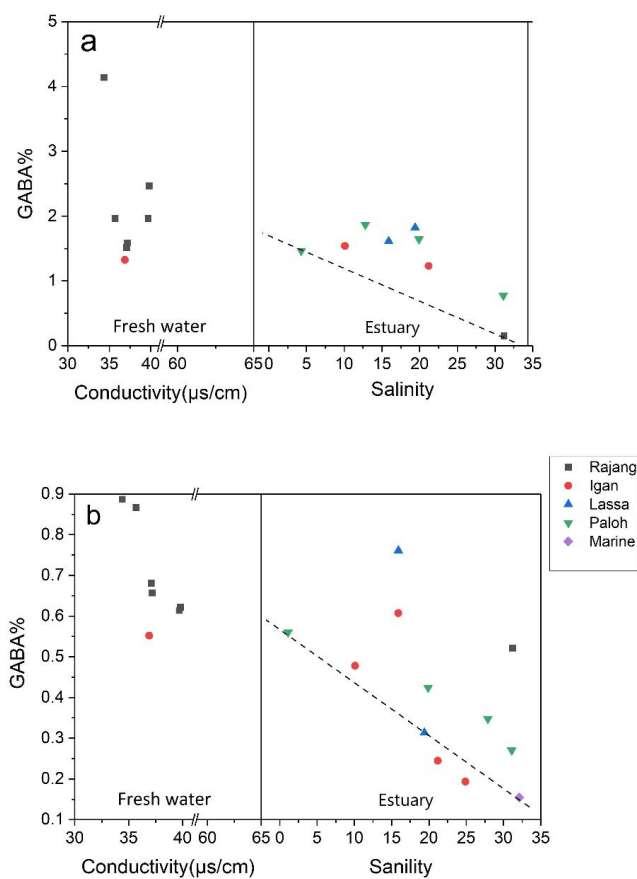
579

580 Figure 3. Distribution pattern of (a) DOC $\delta^{13}\text{C}$ and (b) POC $\delta^{13}\text{C}$ along with conductivity/salinity
 581 in the Rajang. The legend indicates the branches that the samples were from and marine
 582 corresponds to S1 station.

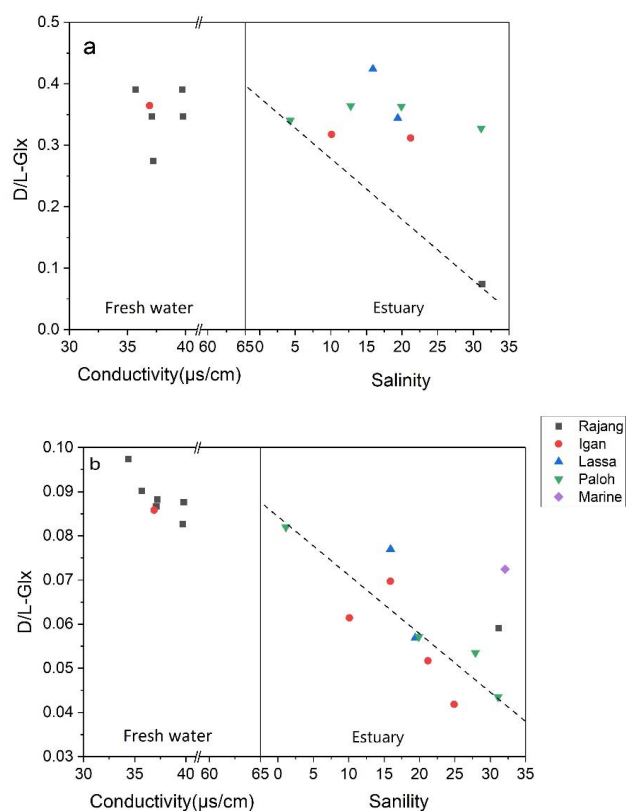
583

584

585



586
 587 Figure 4. GABA% distribution pattern from fresh water to estuary in the Rajang: a) dissolved and
 588 b) particulate. The legend indicates the branches that the samples were from and marine
 589 corresponds to S1 station.
 590
 591



592
 593
 594 Figure 5. D/L ratio of Glx from fresh water to estuary in the Rajang: a) dissolved and b) particulate.
 595 The legend indicates the branches that the samples were from and marine corresponds to S1
 596 station.
 597
 598
 599

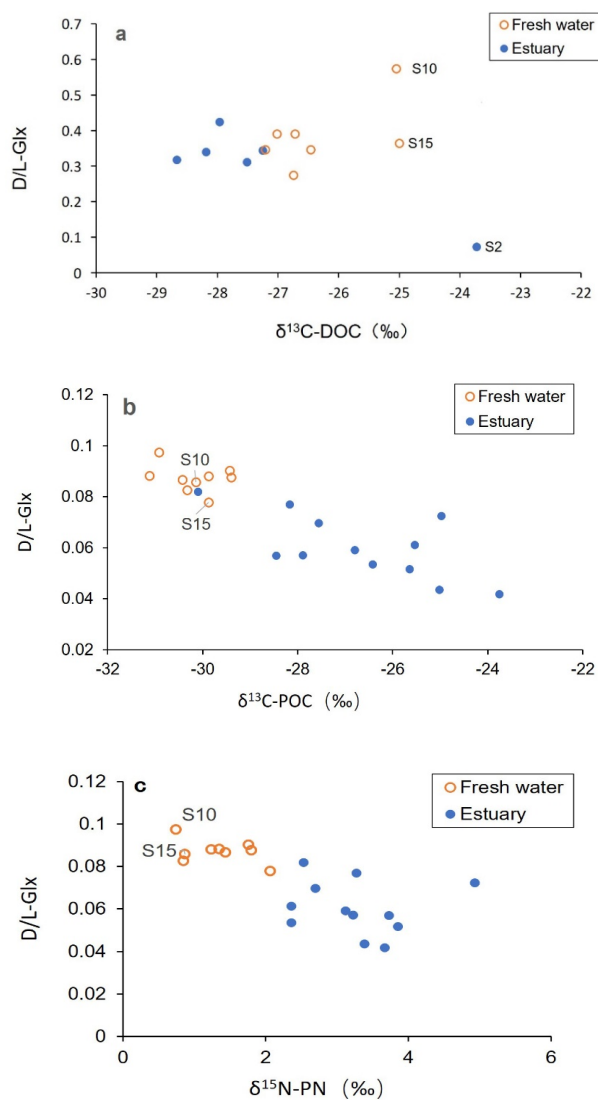
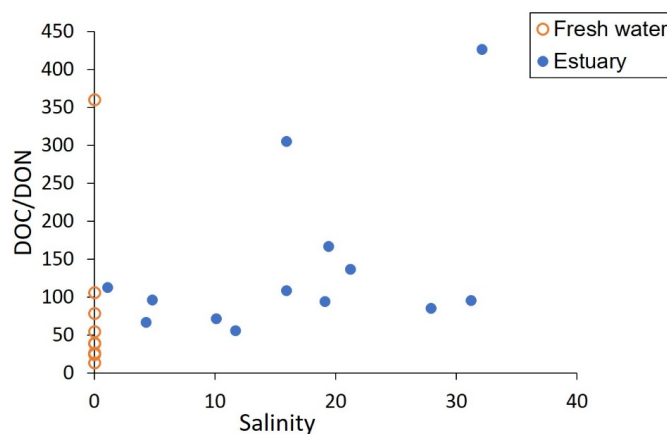
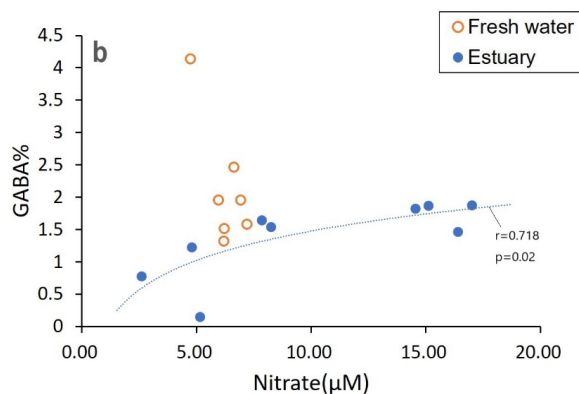
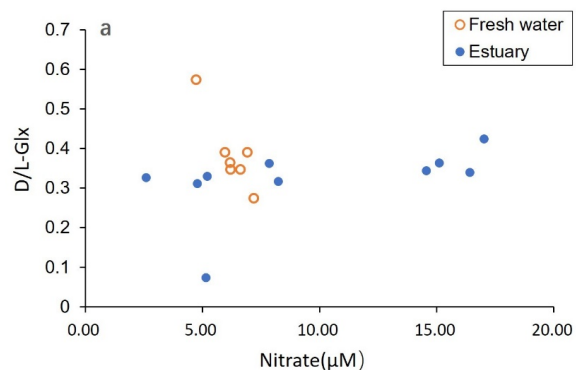


Figure 6. D/L ratio of AAs (as Glx) plotted against a) DOC $\delta^{13}\text{C}$ b) POC $\delta^{13}\text{C}$, and c) PN $\delta^{15}\text{N}$.



608
 609 Figure 7. DOC/DON ratio distribution pattern along with salinity in the Rajang. For fresh water
 610 and estuary, the mean DOC/DON value was 50 and 140, respectively. DON is from Jiang et al.,
 611 (2019)
 612
 613
 614



618

619 Figure 8. Dissolved OM composition (a: D/L Glx, b: GABA%) and its relation with nitrate. Nitrate

620 is derived from Jiang et al., (2019).

621

622